

Published in final edited form as:

Am J Physiol Cell Physiol. 2008 May ; 294(5): C1288–C1297. doi:10.1152/ajpcell.00033.2008.

Calmodulin in adult mammalian skeletal muscle: localization and effect on sarcoplasmic reticulum Ca²⁺ release

George G. Rodney

Department of Organizational Systems & Adult Health, University of Maryland School of Nursing, Baltimore, Maryland

Abstract

Calmodulin is a ubiquitous Ca²⁺ binding protein that binds to ryanodine receptors (RyR) and is thought to modulate its activity. Here we evaluated the effects of recombinant calmodulin on the rate of occurrence and spatial properties of Ca²⁺ sparks as an assay of activation in saponin-permeabilized mouse myofibers. Control myofibers exhibited a time-dependent increase and subsequent decrease in spark frequency. Recombinant wild-type calmodulin prevented the time-dependent appearance of Ca²⁺ sparks and decreased the derived Ca²⁺ flux from the sarcoplasmic reticulum during a spark by ~37%. A recombinant Ca²⁺-insensitive form of calmodulin resulted in an instantaneous increase in spark frequency as well as an increase in the derived Ca²⁺ flux by ~24%. Endogenous calmodulin was found to primarily localize to the Z-line. Surprisingly, removal of endogenous calmodulin did not alter the time dependence of Ca²⁺ spark appearance. These results indicate that calmodulin may not be essential for RyR1-dependent Ca²⁺ release in adult mammalian skeletal muscle.

Keywords

ryanodine receptor; calcium sparks; calcium-induced calcium release; calcium signaling; calcium imaging

In vertebrate skeletal muscle, depolarization of the sarcolemma travels deep into the muscle fiber via sarcolemmal invaginations called the transverse tubules (t-tubules). Activation of the dihydropyridine receptor (DHPR), a voltage-dependent Ca²⁺ channel within the t-tubule, results in Ca²⁺ release from the sarcoplasmic reticulum (SR) through a process termed excitation-contraction coupling (ECC). Ca²⁺ is released from the SR through a large homotetrameric protein in the SR membrane, the ryanodine receptor (RyR). In mammals three RyR isoforms exist (RyR1–3), with the primary isoform in adult skeletal muscle being RyR1 (41) and a small amount (1–5%) of RyR3 in specific muscles such as the diaphragm and soleus (8,21). In addition to the regulation by the DHPR, RyR1 also binds and is thought to be regulated by numerous endogenous molecules, including the Ca²⁺-binding protein calmodulin (CaM).

One molecule of CaM is bound to each RyR1 monomer at both nanomolar and micromolar levels of Ca²⁺, for a total of four CaM molecules per RyR1 tetramer (29). In *in vitro* SR vesicle preparations CaM displays Ca²⁺ dependence in its functional effects on RyR1. At nanomolar levels of free Ca²⁺, Ca²⁺-free CaM sensitizes RyR1 to activation, whereas at micromolar levels of free Ca²⁺, Ca²⁺ CaM inhibits RyR1 (35). Using a mutant CaM that cannot bind Ca²⁺ (CaM₁₂₃₄), Rodney et al. (35) showed that Ca²⁺ binding to CaM converts CaM from an

activator to an inhibitor of RyR1 in SR vesicles and planar lipid bilayers. These studies suggested that CaM does not simply sensitize RyR1 to Ca^{2+} but that CaM senses changes in intracellular Ca^{2+} concentration ($[\text{Ca}^{2+}]_i$), transducing these changes into functional alterations of RyR1. Recently, Yamaguchi et al. (48) have shown that similar to RyR1, RyR3 has a single conserved binding site for CaM. However, under low $[\text{Ca}^{2+}]_i$, CaM activates RyR3 to a greater extent than RyR1; providing evidence for isoform-dependent regulation of RyR by CaM.

In muscle, localized discrete elevations in myoplasmic $[\text{Ca}^{2+}]_i$, Ca^{2+} sparks (5,25), arise from the opening of clusters of RyR channels. It is well established that these Ca^{2+} sparks provide a sensitive assay of the activation and modulation of RyR in a quasiphysiological setting. In permeabilized depolarized frog skeletal muscle, spontaneous Ca^{2+} sparks are initiated by ligand activation and are terminated by inactivation of RyR; with both being independent of the voltage sensor (25). Using Ca^{2+} sparks as an assay to monitor RyR function within frog skeletal muscle, we have previously reported that exogenously applied recombinant CaM localized to the triad and caused a highly cooperative dose-dependent increase in Ca^{2+} spark frequency (36). However, we did not observe any changes in the spatial and temporal properties of the release events, suggesting that Ca^{2+} binding to exogenous CaM does not participate in Ca^{2+} spark termination. To gain further insight into the CaM modulation of RyR-dependent SR Ca^{2+} release, we now extend our work to a mammalian preparation. Unlike the frog, intact adult mammalian myofibers do not produce voltage-activated Ca^{2+} sparks. This difference may be due to the presence of RyR β (3) in the frog (27,31,46). It is well accepted, however, that although Ca^{2+} sparks occur less frequently in permeabilized mammalian myofibers, they remain a robust reliable assay of RyR1 function (10,19,24,44,45,50). Therefore, we examined the effect of CaM on Ca^{2+} sparks in permeabilized adult mouse myofibers. Recombinant CaM resulted in a time-dependent alteration of Ca^{2+} sparks. Surprisingly, removal of endogenous CaM did not alter the occurrence of Ca^{2+} sparks, whereas immunofluorescence localization of endogenous CaM suggests that the triad may not be the predominant locus for CaM within the myofiber. These results indicate that CaM may not be essential for RyR1-dependent Ca^{2+} release in adult mammalian skeletal muscle.

MATERIALS AND METHODS

Fiber preparation

Adult CD-1 mice (Charles River) were killed by CO_2 asphyxiation in accordance with the National Institutes of Health guidelines and were approved by the Institutional Animal Care and Use Committee of the University of Maryland, Baltimore, MD. Diaphragm and flexor digitorum brevis (FDB) muscles were dissected and enzymatically dissociated with either a combination of collagenase A (2 mg/ml, Roche) and Dispase II (6 mg/ml, Roche) (diaphragm) or collagenase A (2 mg/ml) alone (FDB) dissolved in essentially Ca^{2+} -free HEPES-buffered rodent Ringer solution containing (in mM) 146 NaCl, 4.7 KCl, 0.6 MgSO_4 , 1.6 NaCO_3 , 0.13 NaH_2PO_4 , 7.8 glucose, 20 HEPES, pH 7.3 supplemented with 10% fetal bovine serum (FBS, Biofluids) at 37°C for 1.5–2.5 h. Fiber bundles were then transferred to Ca^{2+} -free HEPES-buffered Ringer containing 10% FBS without collagenase or dispase II, teased apart, and separated by gentle trituration. The solution was then changed to Eagle's minimum essential medium with Earle's salts (GIBCO) containing 10% FBS and 100 μM gentamicin (Sigma). Intact single fibers were plated on extracellular matrix (Sigma)-coated coverslips attached across a 15-mm hole in the bottom of 35-mm petri dishes (MatTek) in serum-supplemented medium. Isolated myofibers were incubated overnight in a 5% CO_2 incubator at 37°C in serum-supplemented medium to allow retention of only viable fibers. Experiments were conducted on myofibers 24–48 h after plating was completed.

Calcium imaging

Chemical permeabilization of the sarcolemma was achieved with saponin (12 $\mu\text{g/ml}$; 2–3 min) in internal solution containing (in mM) 90 K-sulfate, 10 creatine phosphate, 5 Na-ATP, 5 glucose, 0.1 EGTA, 7 Mg^{2+} , 10 HEPES, and 0.05 Fluo-4 pentapotassium salt. Fibers were then exposed to an internal solution containing 0.05 mM Fluo-4 with or without CaM or CaM₁₂₃₄ (2 μM) before image acquisition. The free $[\text{Ca}^{2+}]_i$ was calculated to be 100 nM using MAXC v2.5 (1).

Fibers were imaged for spontaneous Ca^{2+} sparks on an inverted microscope (Olympus IX-71 with a $\times 60$, 1.3 numerical aperture water-immersion objective) coupled to a Bio-Rad CellMap IC laser scanning confocal imaging system. A sequence of 40 XY images was collected over time after solution change to either internal solution without any added CaM (control) or an internal solution containing recombinant drosophila CaM (dCaM), either wild-type dCaM (2 μM), or dCaM₁₂₃₄ (2 μM). The frequency of sparks was determined by using a modified automatic detection method as previously described (6). Briefly, an average fiber fluorescence image was generated by calculating the mean fluorescence pixel by pixel of all 40 XY images. The region of the image corresponding to the fiber was manually defined as an area of interest, and potential local Ca^{2+} sparks were identified as contiguous pixels exhibiting fluorescence ≥ 1.5 SD above the mean fiber fluorescence. Regions selected as local Ca^{2+} events were identified in $\Delta\text{F}/\text{F}$ images as contiguous regions of pixels having fluorescence values ≥ 2 SD above the mean fluorescence and were selected by the criterion that at least 1 pixel within the 2 SD area must exceed 3 SD above the mean. Ca^{2+} sparks were characterized in the $\Delta\text{F}/\text{F}$ image by the measured parameters peak amplitude (peak $\Delta\text{F}/\text{F}$) and full area at half-maximal fluorescence (FAHM; μm^2) and by the derived parameters of equivalent diameter (EDHM; μm) and equivalent volume integral (VIHM; $\mu\text{m}^3 \cdot \Delta\text{F}/\text{F}$) at half-maximal fluorescence as previously detailed by Chun et al. (6).

Localization of recombinant CaM

Localization of recombinant CaM in saponin-permeabilized fibers was performed using Alexa Fluor 488 (Molecular Probes, Eugene, OR) labeled mammalian CaM (mCaM488, 1 μM) in conjunction with labeling of the actin cytoskeleton with Texas Red-X phalloidin (775 nM, Molecular Probes) for 20 min in internal solution as previously described (36). Alexa Fluor 488 is a 643-Da succinimidyl ester that is conjugated to the NH_2 -terminus of CaM.

Immunofluorescence localization of endogenous CaM

Myofibers were fixed with 4% paraformaldehyde in PBS for 10 min, washed three times with PBS, and permeabilized in 0.1% Triton for 10 min. Fibers were then incubated in 8% goat serum (Jackson Immuno-Research) for 1 h at 4°C. Fibers were incubated overnight at 4°C with a monoclonal antibody against CaM (mouse anti-calmodulin, Zymed) in 2% goat serum followed by labeling with an Alexa488-conjugated goat anti-mouse secondary antibody (Molecular Probes). Fibers were then washed three times with PBS and blocked with 8% donkey serum followed by incubation with the indicated primary antibody overnight. Myofibers were then washed three times with PBS containing 2% serum (donkey or goat) at room temperature, followed by incubation with either Cy5- or Alexa635-conjugated anti-mouse or anti-rabbit IgG overnight at 4°C. Images were acquired on either a Olympus FV500 or a Zeiss 510 fluorescent laser scanning confocal microscope. Secondary antibody labeling showed no detectable fluorescence pattern. For colocalization analysis, two-dimensional (X-Y) images were acquired sequentially so as to prevent spectral bleed through.

Data analysis

Data are reported as means \pm SE, unless otherwise specified. Statistical analysis was performed in Sigma Stat (Jandel) with a significance level of $P < 0.05$. Colocalization analysis was performed in Volocity (Improvision).

RESULTS

The observation that spontaneous Ca^{2+} sparks do occur in permeabilized mammalian skeletal muscle (24) affords us the opportunity to study the effects of putative protein modulators of RyR1 on the SR Ca^{2+} release process in mammalian cells. In these studies Ca^{2+} sparks were used as a tool to assess the role of CaM in modulating RyR1 function in situ while immunofluorescence studies were undertaken to localize endogenous CaM in mammalian skeletal muscle.

Effect of dCaM on spontaneous Ca^{2+} sparks

Figure 1A shows representative $\Delta\text{F}/\text{F}$ images of Ca^{2+} sparks in saponin-permeabilized diaphragm myofibers in the presence of buffer (Control), wild-type dCaM, and dCaM1234. A detailed analysis revealed that peak Ca^{2+} spark occurrence was at 394 ± 28 s, followed by a decrease (Fig. 1B). Because of the time required for buffer exchange between control solutions and test solutions (e.g., wild-type dCaM or dCaM₁₂₃₄) and this time-dependent appearance of Ca^{2+} sparks, experiments were conducted under conditions in which the test solution was not paired with a control recording. In other words, after removal of the saponin solution the fiber was exposed to internal solution containing either control buffer, dCaM, or dCaM₁₂₃₄. Incubation of diaphragm fibers with wild-type dCaM (2 μM) effectively suppressed the time-dependent increase in spark frequency, the Ca^{2+} spark frequency remained relatively constant and low throughout the recording (Fig. 1B). dCaM₁₂₃₄ (2 μM), however, resulted in an increase in spark frequency at practically all time points compared with all other conditions tested. The time-to-peak Ca^{2+} spark occurrence was also shifted in the presence of dCaM₁₂₃₄ compared with controls (516 ± 44 vs. 394 ± 28 s, respectively, Fig. 1B). Figure 1C shows that on average over the entire recording time dCaM₁₂₃₄ increased Ca^{2+} spark frequency by 169% when compared with controls. The events that occur under these conditions result from voltage-independent SR Ca^{2+} release, and therefore, these data support the hypothesis that Ca^{2+} -free CaM sensitizes RyR1 to Ca^{2+} -induced Ca^{2+} release (CICR).

Assessment of the spatial parameters of Ca^{2+} sparks provides an estimate for the effect of wild-type dCaM and dCaM₁₂₃₄ on the amount of Ca^{2+} released during a spontaneous Ca^{2+} release event. When compared with control, wild-type dCaM slightly increased (+4.5%) the peak amplitude ($\Delta\text{F}/\text{F}$) but significantly decreased (-36.7%) the volume integral (i.e., mass) of Ca^{2+} release (Fig. 2A, Table 1). dCaM₁₂₃₄ increased the spatial and mass parameters of the release events compared with controls. There was a 24.3% increase in $\Delta\text{F}/\text{F}$ and a 24.4% increase in the volume integral (Fig. 2B, Table 1). Taken together, these data indicate that wild-type dCaM reduces the likelihood of eliciting SR Ca^{2+} release, whereas dCaM₁₂₃₄ sensitizes RyR1 to open. The observed changes in VIHM could represent alterations in the amount of Ca^{2+} released; i.e., wild-type dCaM decreasing and dCaM₁₂₃₄ increasing the amount of Ca^{2+} released. Alternatively, the decrease in VIHM with wild-type dCaM may represent an increase in Ca^{2+} buffering within the myoplasm.

Previously, in amphibian skeletal muscle, wild-type dCaM increased Ca^{2+} spark frequency (36), just the opposite of what was observed in the present studies. Both amphibian skeletal muscle and mammalian diaphragm express RyR1 and RyR3, although diaphragm expresses RyR3 to a much lesser extent. To further investigate the differences observed between amphibian muscle and mammalian diaphragm, the effect of wild-type dCaM on Ca^{2+} spark

frequency was examined in a mammalian fast-twitch muscle that expresses only RyR1 (e.g., FDB). Figure 3 shows that wild-type dCaM decreased Ca^{2+} spark frequency while dCaM₁₂₃₄ increased Ca^{2+} spark frequency in FDBs. When compared with the diaphragm, wild-type dCaM was much more effective in inhibiting Ca^{2+} sparks, whereas dCaM₁₂₃₄ was much less effective at activating Ca^{2+} sparks. Since amphibian skeletal muscle contains equal proportions of RyR1 and RyR3 (α and β , respectively) while mammalian skeletal muscle expresses little (diaphragm) to no (FDB) RyR3, these data suggest that CaM shows isoform specificity in modulation of SR Ca^{2+} release.

Kinetics and localization of exogenous CaM

To assess the kinetics of CaM binding within the permeabilized myofiber, the diffusion of fluorescently labeled recombinant CaM (mCaM488) was assessed. Figure 4A shows the time course for washin of mCaM488 (1 μM) immediately after permeabilization. The data represent the fluorescence within the myofiber after subtraction of background fluorescence, which includes free mCaM488. These data were best fit by a double exponential, with a first phase time constant (τ_1) of 1.9 ± 1.1 min and a second phase time constant (τ_2) of 12.0 ± 2.6 min. The dissociation of mCaM488 from the myofiber was also assessed. Permeabilized myofibers were incubated with mCaM488 (1 μM) for 45 min, without imaging, to reach steady state as determined in Fig. 4A. The bathing solution was then changed to an internal solution without mCaM488 every 5 min for 20 min. Images were acquired immediately after the first solution change and periodically for 35 min. Figure 4B shows the time course of washout of mCaM488. The data were best fit by a single exponential, with a time constant (τ_{off}) of 7.8 ± 0.1 min and an offset of 0.55 ± 0.002 , indicating that only 45% of the bound mCaM488 dissociates from the myofiber.

To assess the localization of recombinant CaM, permeabilized myofibers were double labeled with mCaM488 and Texas Red-X phalloidin. Figure 5 shows that the exogenously added mCaM localizes to the edge of the phalloidin band. Fourier analysis defined a repeating intensity with a long-axis spacing of 0.99 μm for mCaM488 and 1.98 μm for phalloidin. Colocalization analysis shows that mCaM488 and phalloidin do not colocalize within the muscle fiber (Table 2). Given that phalloidin localizes to the I-band in skeletal muscle (3), these data suggest that the exogenously added recombinant CaM localizes primarily to the triad, the site of RyR-mediated SR Ca^{2+} release.

Endogenous CaM localizes to the Z-line

To determine the precise location of endogenous CaM within the muscle fiber, double immunofluorescence labeling was performed for CaM and for either α -actinin, RyR, or inositol trisphosphate receptors (IP_3R). Labeling of endogenous CaM showed a transverse sarcomeric pattern (Fig. 6a) with a long-axis spacing of 1.96 μm . The peak in the anti-CaM fluorescence aligned with the peak in the anti- α -actinin fluorescence (Fig. 6, b–d). Colocalization analysis confirms that endogenous CaM colocalizes with α -actinin (i.e., Z-lines) in mouse diaphragm muscle (Table 2). The peak in the CaM fluorescence pattern aligned with every other RyR fluorescence minima (i.e., between every other RyR doublet) in both diaphragm (Fig. 6B) and FDB (Fig. 6D) myofibers. Fourier analysis resulted in a long-axis spacing of 1.82 and 0.91 μm in the diaphragm and 2.03 and 1.10 μm in the FDB for CaM and RyR, respectively. Colocalization analysis indicates that the CaM does not colocalize with RyR (Table 2). Figure 6C shows that CaM colocalizes with IP_3R . The peak in the CaM fluorescence pattern aligns with the peak in the IP_3R fluorescence pattern, with a long-axis spacing of 1.82 μm for both CaM and IP_3R . Colocalization analysis indicates that CaM and IP_3R colocalize in adult mammalian skeletal muscle (Table 2). Since in mammalian skeletal muscle the triad is located at the end of the A-band (12,42) and not at the Z-line, these data suggest that endogenous CaM

is primarily located at sites away from the sites for RyR-dependent SR Ca^{2+} release, notably the Z-line.

The time-dependent increase in Ca^{2+} spark frequency and the inhibitory effect of wild-type recombinant dCaM may reflect dissociation of endogenous CaM upon permeabilization of the myofiber. Two approaches were taken to test this possibility. First, immunolocalization of CaM was performed in myofibers that had been saponin permeabilized and bathed in internal control solution for 30 min before fixation. Figure 7A shows that the permeabilization protocol used for Ca^{2+} spark measurements does not result in an appreciable loss of endogenous CaM. Furthermore, immunolocalization of α -actinin in the same cell (Fig. 7B) shows that endogenous CaM colocalizes with α -actinin and thus remains localized to the Z-line (Fig. 7, C–D; Table 2). The second approach was to use the myosin light chain kinase (MLCK) CaM binding peptide to promote CaM dissociation. The MLCK CaM binding peptide (10 μM) promoted dissociation of CaM from the myofiber (Fig. 8, A–B); however, no significant effect on the time course of Ca^{2+} spark frequency was observed compared with controls (Fig. 8D). Taken together, these data indicate that dissociation of endogenous CaM does not play a significant role in the time course of Ca^{2+} spark appearance.

DISCUSSION

RyRs are a family of intracellular channels that regulate the release of Ca^{2+} from the SR. Over the last several decades there has been accumulating evidence that CaM is a potent modulator of RyR function. In vitro studies have suggested that CaM activates RyR1 and RyR3 at low Ca^{2+} concentrations ($<1 \mu\text{M}$) and inactivates these channels at elevated Ca^{2+} concentrations ($>1 \mu\text{M}$) (4,35,38). Both Ca^{2+} -free CaM and Ca^{2+} -CaM have been shown to bind to a single overlapping site within residues 3614–3643 of RyR1 (29) or residues 3467–3498 of RyR3 (48). Mutations within the 3614–3643 CaM binding site (L3624D and W3620A) disrupted the interaction of CaM with RyR1 (49) as assessed by in vitro binding assays. Interestingly, expression of L3624D or W3620A mutant RyR1 channels in dyspedic skeletal myotubes restored ECC (30), suggesting that CaM binding to the 3614–3643 CaM-binding region of RyR1 is not essential for voltage-activated SR Ca^{2+} release. More recently, using permeabilized adult frog skeletal muscle fibers, our group (36) has shown that exogenously applied recombinant dCaM activated RyR, as measured by an increase in Ca^{2+} spark frequency. Taken together, these studies indicate that the role of CaM in modulating SR Ca^{2+} release in skeletal muscle is equivocal.

In the present study, the role of CaM in modulating RyR-dependent SR Ca^{2+} release in mammalian skeletal muscle was investigated. To this end, we assayed spontaneous SR Ca^{2+} release (i.e., Ca^{2+} sparks) in adult permeabilized mammalian skeletal muscle fibers. Here we report that recombinant wild-type dCaM decreased the time-dependent increase in Ca^{2+} spark occurrence and the derived volume integral of Ca^{2+} released during a spark, whereas dCaM₁₂₃₄ (Ca^{2+} -free CaM) increased Ca^{2+} spark frequency as well as the volume integral of Ca^{2+} released. These data support the premise that CaM is a modulator of RyR-dependent SR Ca^{2+} release.

Permeabilized myofibers showed a time-dependent increase in Ca^{2+} sparks that was blocked by recombinant wild-type dCaM and enhanced by the Ca^{2+} -binding mutant dCaM₁₂₃₄ (Fig. 1). This transient nature of Ca^{2+} sparks in skeletal muscle following membrane permeabilization has been attributed to an excess production of reactive oxygen species (18, 19), with minor contributions coming from changes in SR Ca^{2+} content (26,34). Whether the observed effects of dCaM on Ca^{2+} spark appearance in the present study result from alterations in the redox potential of the cell (e.g., CaM-dependent nitric oxide synthase) or through alterations in SR Ca^{2+} content are uncertain. Since in skeletal muscle, unlike cardiac muscle,

store depletion appears to be a weak modulator of SR Ca^{2+} release (34), CaM-dependent changes in SR Ca^{2+} content are less likely.

The time-dependent increase in Ca^{2+} sparks might reflect dissociation of endogenous CaM from RyR1 upon permeabilization and that exogenous CaM may act by replacing endogenous CaM at the same inhibitory site. The action of dCaM₁₂₃₄ (Fig. 1) and the finding that the time course for the binding and dissociation of mCaM488 (Fig. 4) are on the same order of magnitude as the appearance of Ca^{2+} sparks are all consistent with this possibility. However, permeabilization of the myofiber did not result in an appreciable loss nor an alteration in the localization of endogenous CaM (Fig. 7), arguing against dissociation of endogenous CaM as the reason for the increase in Ca^{2+} sparks under these conditions. Furthermore, removal of endogenous CaM with MLCK CaM binding peptide did not significantly alter the time dependence of Ca^{2+} spark occurrence (Fig. 8). Thus the most likely explanation for the alteration of Ca^{2+} sparks in permeabilized mammalian skeletal myofibers is that the recombinant CaM is binding to sites not occupied by endogenous CaM, analogous to that proposed for permeabilized frog skeletal muscle (36).

Interestingly, in the present study wild-type dCaM decreased Ca^{2+} spark frequency, whereas in amphibian skeletal muscle wild-type dCaM activated Ca^{2+} sparks (36). Amphibian skeletal muscle expresses equal proportions of RyR1 and RyR3, whereas adult mammalian skeletal muscle expresses little, <1% of total RyR is composed of RyR3 (diaphragm), to no RyR3 (FDB). Thus the ability of CaM to activate Ca^{2+} sparks in amphibian skeletal muscle but inhibit Ca^{2+} sparks in adult mammalian skeletal muscle suggests a differential modulation of RyR1 versus RyR3 by CaM as previously suggested (13,17,48). The differential efficacy for inhibition of Ca^{2+} sparks by wild-type dCaM and activation of Ca^{2+} sparks by dCaM₁₂₃₄ between diaphragm and FDB myofibers (Fig. 3) could also be explained by an isoform-dependent modulation of SR Ca^{2+} release by CaM. Understanding the mechanisms for this differential regulation is important, as developing mammalian skeletal muscle expresses equal proportions of RyR1 and RyR3 and thus CaM may play a key role in Ca^{2+} signaling during myofiber development. Studies addressing this hypothesis are underway.

What might prevent endogenous CaM from associating with RyR in skeletal muscle? Recent data has suggested that the CaM binding site of RyR1 (amino acids 3614–3643) also interacts with a CaM-like domain of RyR1 (amino acids 4064–4210), suggesting that the CaM binding site is involved in an intramolecular interaction (14,47). The CaM binding domain of RyR1 may also be a site for an intermolecular interaction with $\text{Ca}_v1.1$ (DHPR) in the t-tubule membrane (15,39). Recently, Schneider and colleagues (33) have suggested that S100A1 modulates SR Ca^{2+} release. In those studies the authors show that in FDB fibers lacking S100A1, the voltage-activated global Ca^{2+} transient is depressed. Furthermore, they provide evidence that S100A1 binds to the amino terminal portion of the previously identified CaM binding site (29) and competes with CaM for this binding site. It is not known whether in the current study wild-type CaM displaces bound S100A1 from RyR1, resulting in inhibition of RyR1. The observation that wild-type recombinant dCaM reduced the volume integral of Ca^{2+} release in the present study would be consistent with this possibility. Additional studies are warranted to understand the interplay between CaM and S100A1 in the regulation of RyR-dependent SR Ca^{2+} release. Thus the ability of the CaM binding site of RyR1 to be a site for protein-protein interactions with proteins other than CaM might prevent CaM from associating with RyR in mature intact mammalian skeletal muscle. The finding that recombinant CaM accumulates within the triad suggests that permeabilization of the myofiber disrupts any inter or intramolecular interactions that would normally prevent the association of CaM with RyR. Disruption of the DHPR-RyR1 intermolecular coupling is thought to be a prerequisite for the appearance of spontaneous Ca^{2+} sparks in mammalian skeletal muscle (2), allowing for binding of CaM to RyR1 and modulation of SR Ca^{2+} release. CaM may be localizing to regions away

from the triad through its interactions with cytoskeletal proteins (e.g., dystrophin), IP₃Rs (Fig. 6), and phosphorylase b kinase (22). Harper and colleagues (16) have shown that digestion of glycogen granules with α -amylase greatly reduced the striated staining pattern for CaM. Given that CaM is the δ -subunit of phosphorylase b kinase (7), these data suggest that the localization of CaM may be primarily determined by glycogen.

The results reported in this study do not completely rule out a role of CaM in modulating skeletal muscle SR Ca²⁺ release. CaM may play a role in regulating SR Ca²⁺ release under conditions in which the intermolecular interactions between the DHPR and RyR1 have either not been formed or have been disrupted, such as during skeletal muscle development when the t-tubules have not formed contact with the SR or during times of fiber degeneration/regeneration when the t-tubules are disrupted (2). Stroffekova (40) has recently shown, using skeletal muscle myotubes, that CaM is associated with the DHPR in vivo and mediates Ca²⁺-dependent inhibition of DHPR current. In the present study, endogenous CaM was primarily found to reside at the Z-line; however, ~25% of the peak CaM immunoreactivity can be seen at the level of the triad. It is not known whether this CaM is associated with the DHPR, but the data presented here strongly suggests that this CaM is not regulating RyR-dependent SR Ca²⁺ release. CaM has displayed Ca²⁺-dependent translocation within cells (9,11,43); thus, CaM may respond to changes in intracellular [Ca²⁺]_i and translocate to other regions of the cell. Stimulation of FDB myofibers at either 1 or 10 Hz did not result in nuclear translocation of CaM-yellow fluorescent protein (28). That study, however, did not look at higher frequencies of sustained activity. CaM may modulate SR Ca²⁺ release during levels of sustained activity (i.e., tetanic contractions) when the [Ca²⁺]_i remains elevated. CaM may also regulate Ca²⁺ release via IP₃Rs. IP₃Rs have been localized to the Z-line in skeletal muscle (32,37), and we now show that CaM colocalizes with IP₃Rs (Fig. 6, Table 2). IP₃Rs have been implicated in Ca²⁺ signals that regulate gene expression (20), and recent data suggest that CaM may be constitutively associated with the IP₃R and essential for proper IP₃R function (23). Therefore, it is possible that CaM is interacting with IP₃Rs and is regulating Ca²⁺ signaling involved in cellular functions other than contraction.

In conclusion, the results of this study show that under the conditions used in these experiments exogenous recombinant CaM can modulate RyR function; however, it appears that an alteration of the triadic architecture or an over abundance of CaM, or both, may be necessary to reveal such modulation. The results from O'Connell et al. (30), showing that deletion of the CaM binding region of RyR1 (amino acids 3614–3643) results in no overt change in voltage-dependent SR Ca²⁺ release, together with the results from this study leaves open the question as to what role CaM plays in modulating SR Ca²⁺ release in adult skeletal muscle. Future studies assessing the role of CaM in modulating SR Ca²⁺ release during skeletal muscle development, cycles of degeneration/regeneration, as well as IP₃R-dependent Ca²⁺ release are warranted and will provide critical information to our understanding of the role of CaM in modulating Ca²⁺ signaling in skeletal muscle.

Acknowledgements

The author thanks Dr. Christopher W. Ward for helpful discussions in the preparation of this manuscript.

GRANTS

This work was supported by a Individual National Research Service Award (F32 NS-44636) and a Mentored Research Scientist Development Award (K01 AR-051519-04) from National Institutes of Health to G. G. Rodney.

References

1. Bers DM, Patton CW, Nuccitelli R. A practical guide to the preparation of Ca^{2+} buffers. *Methods Cell Biol* 1994;40:3–29. [PubMed: 8201981]
2. Brown L, Rodney G, Hernandez-Ochoa E, Ward C, Schneider MF. Calcium sparks and T-tubule reorganization in dedifferentiating adult mouse skeletal muscle fibers. *Am J Physiol Cell Physiol* 2006;292:C1156–C1166. [PubMed: 17065203]
3. Bukatina AE, Sonkin BY, Alievskaya LL, Yashin VA. Sarcomere structures in the rabbit psoas muscle as revealed by fluorescent analogs of phalloidin. *Histochemistry* 1984;81:301–304. [PubMed: 6209252]
4. Chen SRW, Li X, Ebisawa K, Zhang L. Functional characterization of the recombinant type 3 Ca^{2+} release channel (ryanodine receptor) expressed in HEK293 cells. *J Biol Chem* 1997;272:24234–24246. [PubMed: 9305876]
5. Cheng H, Lederer WJ, Cannell MB. Calcium sparks: elementary events underlying excitation-contraction coupling in heart muscle. *Science* 1993;262:740–744. [PubMed: 8235594]
6. Chun LG, Ward CW, Schneider MF. Ca^{2+} sparks are initiated by Ca^{2+} entry in embryonic mouse skeletal muscle and decrease in frequency postnatally. *Am J Physiol Cell Physiol* 2003;285:C686–C697. [PubMed: 12724135]
7. Cohen P, Burchell A, Foulkes JG, Cohen PT. Identification of the Ca^{2+} -dependent modulator protein as the fourth subunit of rabbit skeletal muscle phosphorylase kinase. *FEBS Lett* 1978;92:287–293. [PubMed: 212300]
8. Conti A, Gorza L, Sorrentino V. Differential distribution of ryanodine receptor type 3 (RyR3) gene product in mammalian skeletal muscles. *Biochem J* 1996;316:19–23. [PubMed: 8645204]
9. Craske M, Takeo T, Gerasimenko O, Vaillant C, Torok K, Petersen OH, Tepikin AV. Hormone-induced secretory and nuclear translocation of calmodulin: oscillations of calmodulin concentration with the nucleus as an integrator. *PNAS* 1999;96:4426–4431. [PubMed: 10200278]
10. Csernoch L, Zhou J, Stern MD, Brum G, Rios E. The elementary events of Ca^{2+} release elicited by membrane depolarization in mammalian muscle. *J Physiol (Lond)* 2004;557:43–58. [PubMed: 14990680]
11. Deisseroth K, Heist EK, Tsien RW. Translocation of calmodulin to the nucleus supports CREB phosphorylation in hippocampal neurons. *Nature* 1998;392:198–202. [PubMed: 9515967]
12. Franzini-Armstrong C. Simultaneous maturation of transverse tubules and sarcoplasmic reticulum during muscle differentiation in the mouse. *Dev Biol* 1991;146:353–363. [PubMed: 1864461]
13. Fruen BR, Black DJ, Bloomquist RA, Bardy JM, Johnson JD, Louis CF, Balog EM. Regulation of the RYR1 and RYR2 Ca^{2+} release channel isoforms by Ca^{2+} -insensitive mutants of calmodulin. *Biochemistry* 2003;42:2740–2747. [PubMed: 12614169]
14. Gangopadhyay JP, Ikemoto N. Interaction of the K3614-N3643 calmodulin-binding domain with the C4114-N4142 region of the type 1 ryanodine receptor is involved in the mechanism of Ca^{2+} /agonist-induced channel activation. *Biochem J*. 2008 Jan 2; [Epub ahead of print]
15. Gangopadhyay JP, Ikemoto N. Role of the Met3534-Ala4271 Region of the Ryanodine Receptor in the Regulation of Ca^{2+} Release Induced by Calmodulin Binding Domain Peptide. *Biophys J* 2006;90:2015–2026. [PubMed: 16387763]
16. Harper JF, Cheung WY, Wallace RW, Huang HL, Levine SN, Steiner AL. Localization of calmodulin in rat tissues. *Proc Natl Acad Sci USA* 1980;77:366–370. [PubMed: 6987650]
17. Ikemoto T, Takeshima H, Iino M, Endo M. Effect of calmodulin on Ca^{2+} -induced Ca^{2+} release of skeletal muscle from mutant mice expressing either ryanodine receptor type 1 or type 3. *Pflugers Arch* 1998;437:43–48. [PubMed: 9817784]
18. Isaeva EV, Shirokova N. Metabolic regulation of Ca^{2+} release in permeabilized mammalian skeletal muscle fibres. *J Physiol* 2003;547:453–462. [PubMed: 12562922]
19. Isaeva EV, Shkryl VM, Shirokova N. Mitochondrial redox state and Ca^{2+} sparks in permeabilized mammalian skeletal muscle. *J Physiol* 2005;565:855–872. [PubMed: 15845582]
20. Jaimovich E, Carrasco MA. IP_3 dependent Ca^{2+} signals in muscle cells are involved in regulation of gene expression. *Biol Res* 2002;35:195–202. [PubMed: 12415736]

21. Jeyakumar LH, Copello JA, O'Malley AM, Wu GM, Grassucci R, Wagenknecht T, Fleischer S. Purification and characterization of ryanodine receptor 3 from mammalian tissue. *J Biol Chem* 1998;273:16011–16020. [PubMed: 9632651]
22. Jurado LA, Chockalingam PS, Jarret HW. Apocalmodulin. *Physiol Rev* 1999;79:661–682. [PubMed: 10390515]
23. Kasri NN, Torok K, Galione A, Garnham C, Callewaert G, Missiaen L, Parys JB, De Smedt H. Endogenously bound calmodulin is essential for the function of the inositol 1,4,5-trisphosphate receptor. *J Biol Chem* 2006;281:8332–8338. [PubMed: 16410249]
24. Kirsch WG, Uttenweiler D, Fink RHA. Spark- and ember-like elementary Ca^{2+} release events in skinned fibres of adult mammalian skeletal muscle. *J Physiol* 2001;537:379–389. [PubMed: 11731572]
25. Klein MG, Cheng H, Santana LF, Jiang YH, Lederer WJ, Schneider MF. Two mechanisms of quantized calcium release in skeletal muscle. *Nature* 1996;379:455–458. [PubMed: 8559251]
26. Launikonis BS, Zhou J, Santiago D, Brum G, Rios E. The changes in Ca^{2+} sparks associated with measured modifications of intra-store Ca^{2+} concentration in skeletal muscle. *J Gen Physiol* 2006;128:45–54. [PubMed: 16769796]
27. Legrand C, Giacomello E, Berthier C, Allard B, Sorrentino V, Jacquemond V. Spontaneous and voltage-activated Ca^{2+} release in adult mouse skeletal muscle fibres expressing the type 3 ryanodine receptor. *J Physiol* 2008;586:441–457. [PubMed: 18006577]
28. Liu Y, Randall WR, Schneider MF. Activity-dependent and -independent nuclear fluxes of HDAC4 mediated by different kinases in adult skeletal muscle. *J Cell Biol* 2005;168:887–897. [PubMed: 15767461]
29. Moore CP, Rodney G, Zhang JZ, Santacruz-Tolozza L, Strasburg G, Hamilton SL. Apocalmodulin and Ca^{2+} calmodulin bind to the same region on the skeletal muscle Ca^{2+} release channel. *Biochemistry* 1999;38:8532–8537. [PubMed: 10387100]
30. O'Connell KMS, Yamaguchi N, Meissner G, Dirksen RT. Calmodulin binding to the 3614–3643 region of RyR1 is not essential for excitation-contraction coupling in skeletal myotubes. *J Gen Physiol* 2002;120:337–347. [PubMed: 12198090]
31. Pouvreau S, Royer L, Yi J, Brum G, Meissner G, Rios E, Zhou J. Ca^{2+} sparks operated by membrane depolarization require isoform 3 ryanodine receptor channels in skeletal muscle. *Proc Natl Acad Sci USA* 2007;104:5235–5240. [PubMed: 17360329](Erratum in: *Proc Natl Acad Sci USA* 104: 13531, 2007.)
32. Powell JA, Molgo J, Adams DS, Colasante C, Williams A, Bohlen M, Jaimovich E. IP3 receptors and associated Ca^{2+} signals localize to satellite cells and to components of the neuromuscular junction in skeletal muscle. *J Neurosci* 2003;23:8185–8192. [PubMed: 12967979]
33. Prosser BL, Wright NT, Hernandez-Ochoa E, Varney KM, Liu Y, Olojo RO, Zimmer DB, Weber DJ, Schneider MF. S100A1 binds to the calmodulin binding site of ryanodine receptor and modulates skeletal muscle EC coupling. *J Biol Chem* 2008;283:5046–5057. [PubMed: 18089560]
34. Rios E, Launikonis B, Royer L, Brum G, Zhou J. The elusive role of store depletion in the control of intracellular calcium release. *J Muscle Res Cell Motil* 2006;1–14. [PubMed: 16362724]
35. Rodney GG, Williams BY, Strasburg GM, Beckingham K, Hamilton SL. Regulation of RYR1 activity by Ca^{2+} and calmodulin. *Biochemistry* 2000;39:7807–7812. [PubMed: 10869186]
36. Rodney GG, Schneider MF. Calmodulin modulates initiation but not termination of spontaneous Ca^{2+} sparks in frog skeletal muscle. *Biophys J* 2003;85:921. [PubMed: 12885639]
37. Salanova M, Priori G, Barone V, Intravaia E, Flucher B, Ciruela F, McIlhinney R, Parys J, Mikoshiba K, Sorrentino V. Homer proteins and InsP(3) receptors co-localise in the longitudinal sarcoplasmic reticulum of skeletal muscle fibres. *Cell Calcium* 2002;32:193–200. [PubMed: 12379179]
38. Schneider MF, Rodney GG, Ward CW. Local Ca^{2+} release events in skeletal muscle. *J Muscle Res Cell Motil* 2004;25:587–589. [PubMed: 16118845]
39. Sencer S, Papineni RVL, Halling DB, Pate P, Krol J, Zhang JZ, Hamilton SL. Coupling of RYR1 and L-type calcium channels via calmodulin binding domains. *J Biol Chem* 2001;276:38237–38241. [PubMed: 11500484]
40. Stroffekova K. Ca^{2+} /CaM-dependent inactivation of the skeletal muscle L-type Ca^{2+} channel (Cav1.1). *Pflügers Arch* 2008;455:873–884.

41. Sutko JL, Airey JA. Ryanodine receptor Ca^{2+} release channels: does diversity in form equal diversity in function? *Physiol Rev* 1996;76:1027–1071. [PubMed: 8874493]
42. Takekura H, Flucher BE, Franzini-Armstrong C. Sequential docking, molecular differentiation, and positioning of T-Tubule/SR junctions in developing mouse skeletal muscle. *Dev Biol* 2001;239:204–214. [PubMed: 11784029]
43. Thorogate R, Torok K. Ca^{2+} -dependent and -independent mechanisms of calmodulin nuclear translocation. *J Cell Sci* 2004;117:5923–5936. [PubMed: 15522886]
44. Wang X, Weisleder N, Collet C, Zhou J, Chu Y, Hirata Y, Zhao X, Pan Z, Brotto M, Cheng H, Ma J. Uncontrolled calcium sparks act as a dystrophic signal for mammalian skeletal muscle. *Nat Cell Biol* 2005;7:525–530. [PubMed: 15834406]
45. Ward CW, Reiken S, Marks AR, Marty I, Vassort G, Lacampagne A. Defects in ryanodine receptor calcium release in skeletal muscle from postmyocardial infarcted rats. *FASEB J* 2003;17:1517–1519. [PubMed: 12824280]
46. Ward CW, Rodney GG. Does a lack of RyR3 make mammalian skeletal muscle EC coupling a “sparkless” affair? *J Physiol (Lond)* 2008;586:313–314. [PubMed: 18192614]
47. Xiong L, Zhang JZ, He R, Hamilton SL. A Ca^{2+} binding domain in RyR1 that interacts with the calmodulin binding site and modulates channel activity. *Biophys J* 2005;90:173–182. [PubMed: 16227507]
48. Yamaguchi N, Xu L, Pasek DA, Evans KE, Chen SR, Meissner G. Calmodulin regulation and identification of calmodulin binding region of type-3 ryanodine receptor calcium release channel. *Biochemistry* 2005;44:15074–15081. [PubMed: 16274254]
49. Yamaguchi N, Xin C, Meissner G. Identification of apocalmodulin and Ca^{2+} -calmodulin regulatory domain in skeletal muscle Ca^{2+} release channel, ryanodine receptor. *J Biol Chem* 2001;276:22579–22585. [PubMed: 11306590]
50. Zhou J, Brum G, Gonzalez A, Launikonis BS, Stern MD, Rios E. Ca^{2+} sparks and embers of mammalian muscle. Properties of the sources. *J General Physiol* 2003;122:95.

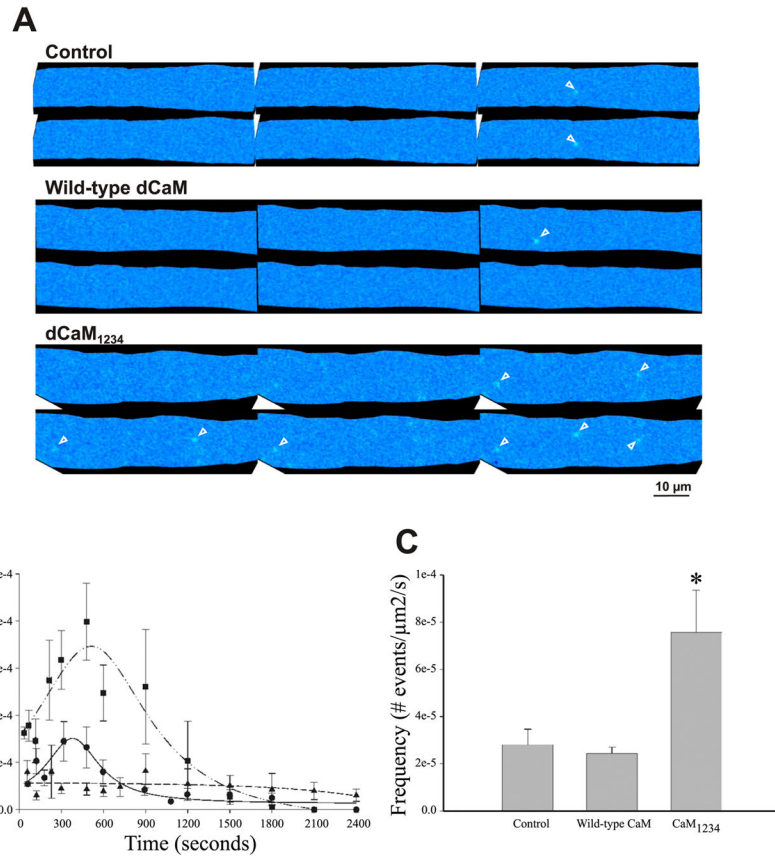


Fig. 1. Effect of wild-type drosophila CaM (dCaM) and a mutant CaM that cannot bind Ca^{2+} (dCaM₁₂₃₄) on the appearance of Ca^{2+} sparks in diaphragm. **A:** representative $\Delta F/F$ images showing the occurrence of Ca^{2+} sparks (arrowheads). **B:** under control conditions (circles) Ca^{2+} spark frequency shows a time-dependent increase, peaking at 394 s. Wild-type dCaM (triangles) decreases the frequency of Ca^{2+} sparks. dCaM₁₂₃₄ (squares) results in an increase in the frequency of Ca^{2+} sparks and a shift in the time of peak frequency to 516 s. **C:** dCaM₁₂₃₄ increases the average frequency of Ca^{2+} spark occurrence by about 169% over the entire recording time. * $P < 0.05$ vs. control and wild-type dCaM.

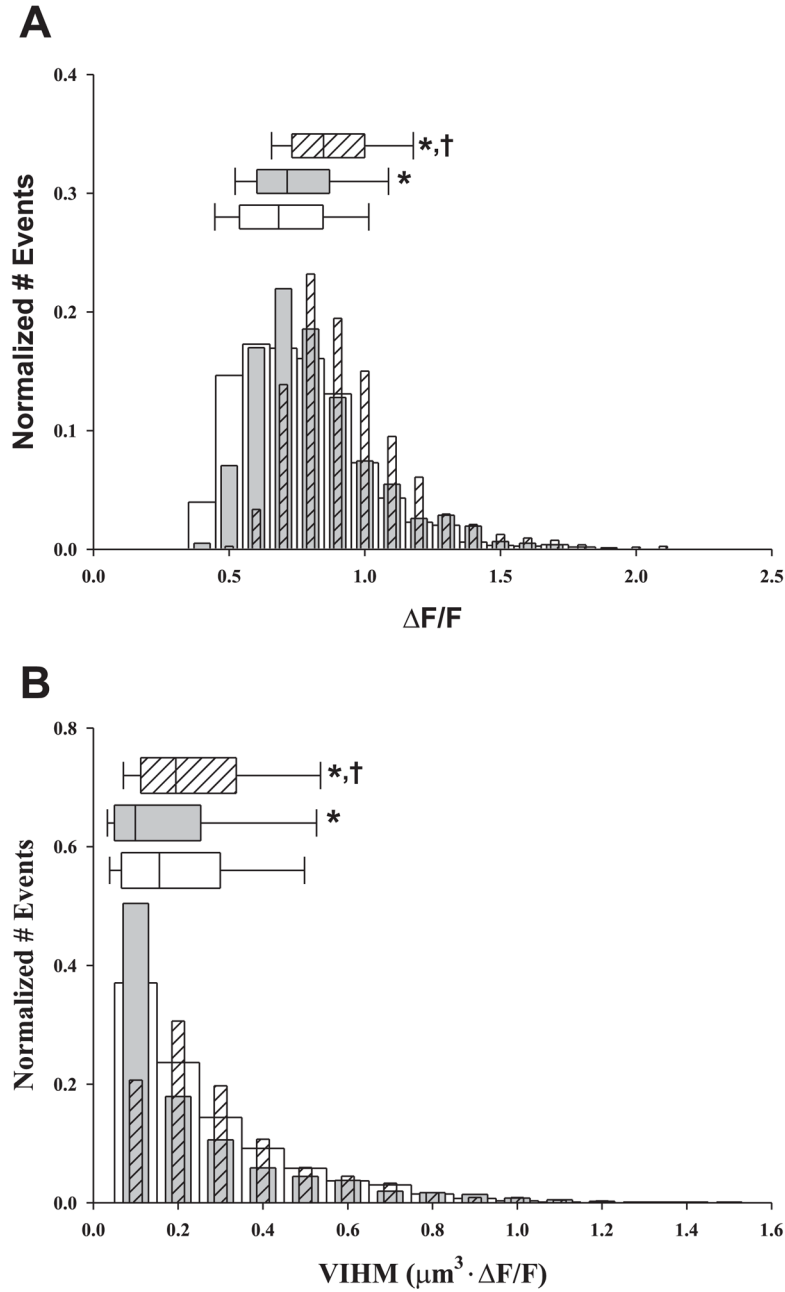


Fig. 2. Effect of dCaM on the spatial properties of Ca^{2+} sparks in diaphragm. Normalized histograms of amplitude (A, $\Delta F/F$) and the derived volume integral at half-maximal fluorescence [B, volume integral half-maximal fluorescence (VIHM); $\mu\text{m}^3 \cdot \Delta F/F$] for controls (open bars, $n_{\text{events}} = 1,481$), wild-type dCaM (gray bar, $n_{\text{events}} = 765$), and dCaM₁₂₃₄ (hatched bar, $n_{\text{events}} = 1,577$). Above each histogram is the median box plot with 25 and 75 (edge of box) and 10 and 90 (error bar cap) percentiles. $P < 0.05$ vs. *control vs. †wild-type dCaM.

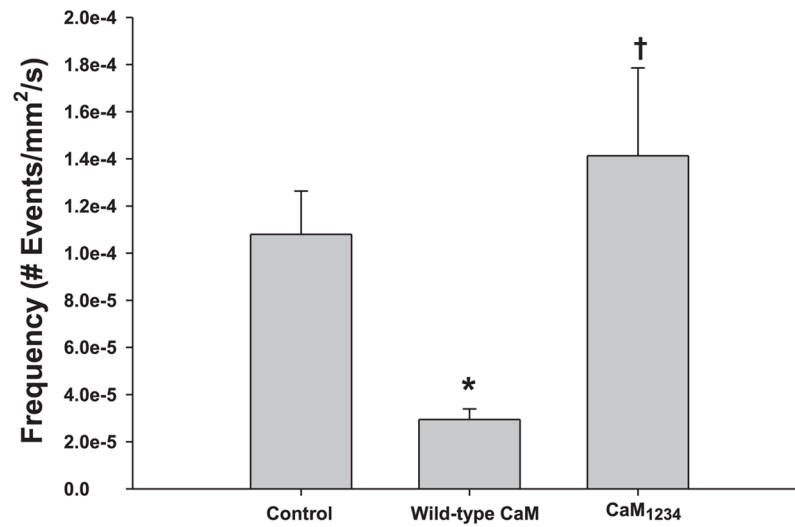


Fig. 3. Effect of dCaM on Ca²⁺ sparks in flexor digitorum brevis myofibers. Wild-type dCaM decreases while dCaM₁₂₃₄ increases average Ca²⁺ spark frequency in myofibers expressing only ryanodine receptor protein (RyR1). $P < 0.05$ vs. *control, vs. †wild-type dCaM.

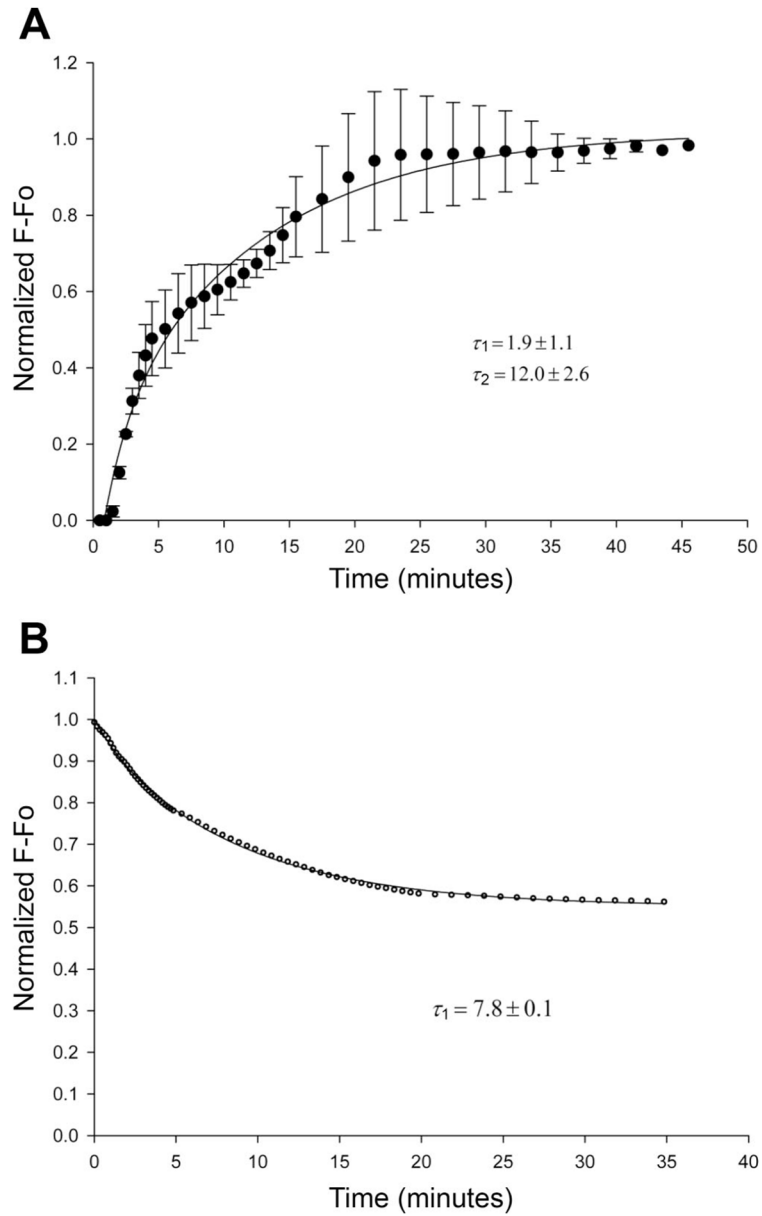


Fig. 4. Diffusion of mammalian CaM (mCaM488) within the diaphragm. *A*: time course for “wash-in” of mCaM488 (1 μ M) immediately after fiber permeabilization. Data were best fit by a double exponential with time constants of 1.9 ± 1.1 and 12.0 ± 2.6 min ($n = 6$ fibers). *B*: time course for “wash-out” of mCaM488 (1 μ M). The binding of CaM488 was allowed to reach equilibrium (45 min) before the start of the “wash-out.” The data were best fit by a single exponential, with a time constant of 7.8 ± 0.1 min and an offset of 0.55 ± 0.002 ($n = 4$ fibers).

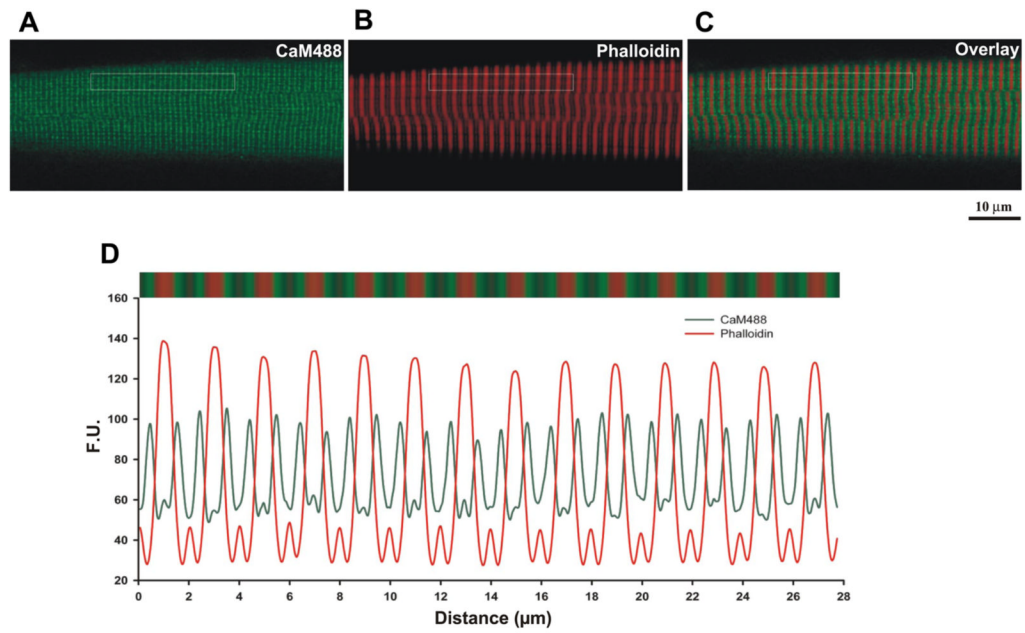


Fig. 5. Recombinant CaM localizes to a region just outside the Z-line in adult diaphragm fibers. *A*: recombinant wild-type mCaM labeled with Alexa488. *B*: Texas Red phalloidin. *C*: overlay image. *D*: spatial profile of the fluorescence pattern indicated in the boxed region from *A* to *C*.

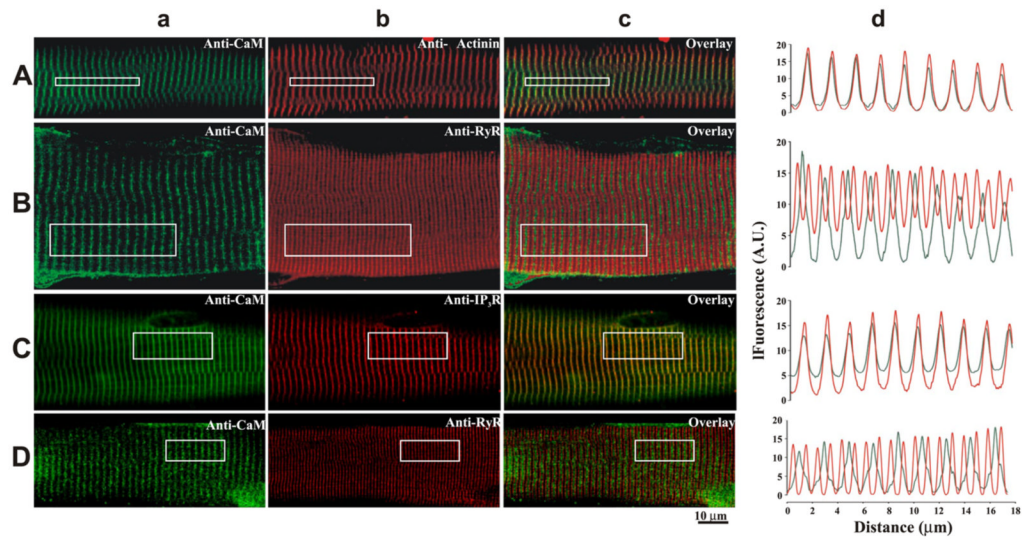


Fig. 6. Localization of endogenous CaM in adult skeletal muscle fibers. Fluorescence confocal images of mouse myofibers from either diaphragm (A–C) or FDBs (D) colabeled with antibodies against CaM (green, Aa–Da) and antibodies against either α -actinin (red, Ab), RyR (red, Bb and Db), and IP₃R (red, Cb). Merged images are shown in Ac–Dc. Spatial profiles of the fluorescence pattern indicated in the boxed region are shown in Ad–Dd.

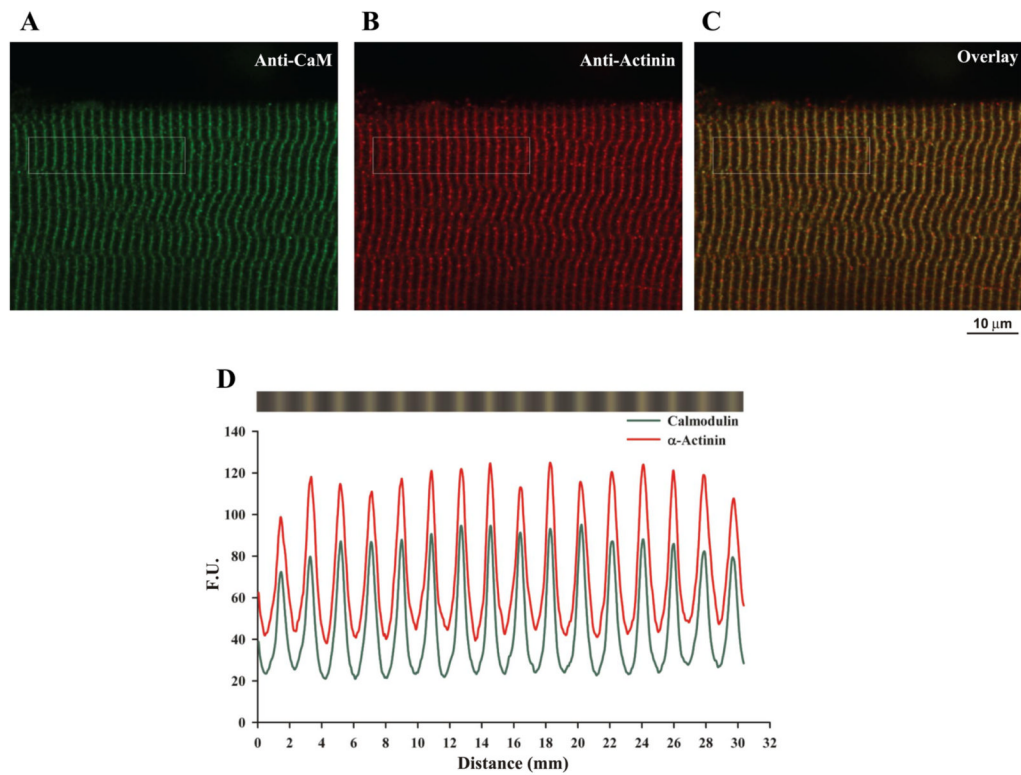


Fig. 7. Endogenous CaM remains localized to the Z-line after permeabilization of adult diaphragm fibers. Fluorescence confocal images of permeabilized mouse diaphragm fibers colabeled with anti-CaM (green, *A*) and anti- α -actinin (red, *B*) antibodies. Merged image is shown in *C*. *D*: spatial profile of the fluorescence pattern indicated in the boxed region from *A* to *C*.

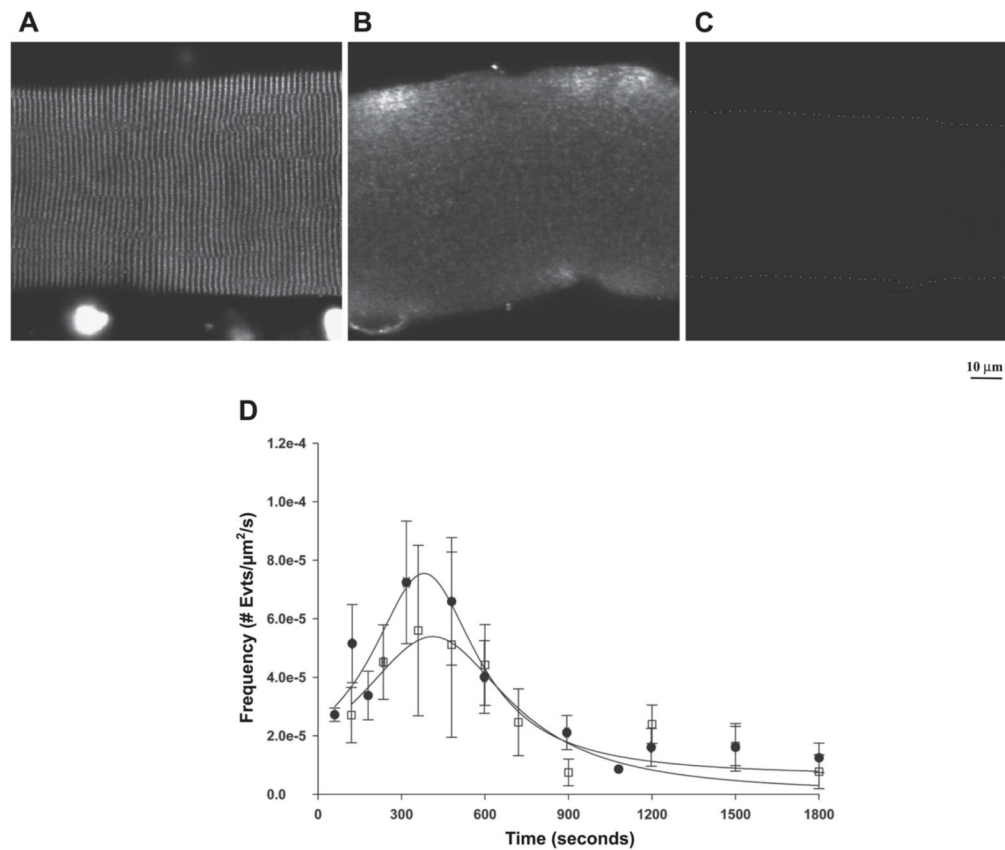


Fig. 8. Effect of a myosin light chain kinase (MLCK) CaM binding peptide on localization of CaM and the time-dependent appearance of Ca²⁺ sparks in diaphragm. Immunofluorescence localization of endogenous CaM shows that the MLCK CaM binding peptide (10 μM) results in a loss of endogenous CaM (A and B). C: no detectable fluorescence from fibers incubated in secondary antibody alone is shown. Dotted line outlines the cell for visual purposes. D: no significant alteration in the appearance of Ca²⁺ sparks was observed in fibers incubated with the MLCK CaM binding peptide (squares) and controls (circles).

Table 1Effect of wild-type dCaM and dCaM₁₂₃₄ on the mean spherical and mass properties of Ca²⁺ sparks in diaphragm muscle

	Amplitude $\Delta F/F$	EDHM, μm	VIHM, μm^3
Control	0.68 (0.54, 0.84)	0.85 (0.66, 1.1)	0.16 (0.07, 0.30)
Wild-type CaM	0.71 (0.60, 0.87) *	0.74 (0.59, 0.97) *	0.10 (0.05, 0.25) *
CaM ₁₂₃₄	0.85 (0.73, 1.0) *, [†]	0.85 (0.72, 1.0) [†]	0.19 (0.11, 0.34) *, [†]

Ca²⁺ spark spatial properties were obtained from *xy* images as described in materials and methods. The values reported are the medians with 25 and 75 percentiles, respectively, in parentheses. CaM, calmodulin; EDHM, equivalent diameter at half-maximal fluorescence.

* $P < 0.05$ vs. control or

[†] wild-type CaM.

Table 2

Colocalization analysis of CaM in adult mammalian diaphragm myofibers

	R	mx	my
CaM488 + phalloidin	0.0513	0.214	0.200
CaM + α -actinin	0.827	0.999	0.999
CaM + RyR	0.199	0.400	0.449
CaM + IP ₃ R	0.793	0.980	0.985
CaM + RyR (FDB)	0.285	0.328	0.368
CaM + α -actinin (permeabilized)	0.928	0.999	0.999

The Pearson's correlation coefficient (R) and colocalization coefficients (*mx*, *my*) were obtained from immunofluorescence images colabeled with the indicated primary antibodies. RyR, ryanodine; IP₃R, inositol trisphosphate receptor; FDB, flexor digitorum brevis.